

Article

# Analysis of Forest Deforestation and its Driving Factors in Myanmar from 1988 to 2017

Rongfeng Yang <sup>1,2,†</sup>, Yi Luo <sup>2,3,\*</sup> , Kun Yang <sup>2,3,†</sup>, Liang Hong <sup>1,2</sup> and Xiaolu Zhou <sup>4</sup>

<sup>1</sup> School of Tourism and Geographical Science, Yunnan Normal University, Kunming 650500, China; yangrongfeng2019@gmail.com (R.Y.); hongliang@ynnu.edu.cn (L.H.)

<sup>2</sup> The Engineering Research Center of GIS Technology in Western China of Ministry of Education of China, Kunming 650500, China; yangkun@ynnu.edu.cn

<sup>3</sup> School of Information Science and Technology, Yunnan Normal University, Kunming 650500, China

<sup>4</sup> Department of Geology and Geography, Georgia Southern University, Statesboro, GA 30485, USA; xzhou@georgiasouthern.edu

\* Correspondence: lysist@ynnu.edu.cn; Tel.: +86-137-0068-3130

† These authors contributed equally to this work.

Received: 8 March 2019; Accepted: 29 May 2019; Published: 29 May 2019



**Abstract:** Myanmar, abundant in natural resources, is one of the countries with high forest cover in Southeast Asia. Along with its rapid socio-economic development, however, the construction of large-scale infrastructure, expansion of agricultural land, and an increasing demand for timber products have posed serious threats to the forests and significantly affected regional sustainable development. However, the geographical environment in Myanmar is complex, resulting in the lack of long-term sequence of land cover data products. Based on 30 years' Landsat satellite remote sensing imagery data and the land cover data extracted by a mixed classification method, this paper examined the spatial and temporal evolution characteristics of forest cover in Myanmar and investigated driving factors of the spatio-temporal evolution. Results show that the forest cover has decreased by 110,621 km<sup>2</sup> in the past 30 years with the annual deforestation rate of 0.87%. Cropland expansion is the main reason for the deforestation throughout the study period. The study can provide basic information of the forest cover data to the Myanmar government for ecological environment protection. At the same time, it can provide important support to the “Belt and Road” initiative to invest in the region's economy.

**Keywords:** forest cover; spatio-temporal change; driving factor; Landsat remote image; Myanmar

## 1. Introduction

The changes, either the increase or decrease, of forest cover can affect the provision of ecosystem services, such as biodiversity abundance, climate regulation, carbon storage and water supply [1–3]. Meanwhile, the transformation of land cover, especially the forest cover, has important implications on the dynamic changes of global change [4–6], as the deforestation is the major driver of climate warming [4,7] and the destruction of biodiversity [4,8]. However, there are limited studies on the quantifications of forest change, although forest ecosystem services are of great importance. Previous studies have been based on samples or have used low spatial resolution, and include studies at the global [9,10], national [11–15], and sub-national scales [16–18]. Nevertheless, in Myanmar, research on forest monitoring and assessment is very scarce, so that this study aims to provide spatial forest cover maps and statistical data of Myanmar. The premise of effectively linking science and policy to forest ecosystems is to strengthen remote sensing monitoring, reporting and verification of forest cover change [19].

The production of satellite data has facilitated the estimation of tropical deforestation. The most commonly used satellite data for monitoring forest changes is the multi-temporal Landsat satellite imagery [20], which data can accurately estimate changes in forest cover [21–25]. Large-scale deforestation in Southeast Asia has attracted much attention in the past few decades [13], due to its strong effects on atmospheric greenhouse gases, biodiversity, and regional climate. Myanmar is one of the countries with the highest forest cover in Southeast Asia [26,27]. Within one of the most globally vulnerable areas, Myanmar's forests and biodiversity are a high conservation priority [28]. The rich forest in Myanmar makes significant contribution to global carbon sequestration, and biodiversity conservation [29]. However, though it still maintains relatively high forest coverage, rapid deforestation and market demand have generated significant impacts on its forest preservation [13]. The major driver for global deforestation is agricultural expansion [30].

In developing countries, investment in agricultural land has grown rapidly over the past two decades [31–33]. Myanmar, Congo and Colombia may be experiencing deforestation driven by rapid agricultural development [34]. The threat of farmland expansion to biodiversity and forest resources needs to be included in effective conservation planning [35]. As a result, to monitor changes in forest cover is important for policy development and implementation.

In this study, based on multi-source and long-time series remote sensing data, Myanmar forest cover data were extracted by a hybrid classification method. We conducted a comprehensive assessment to quantify the patterns of the forest change. By doing so, this study provides average annual forest loss information and verifies that the loss of forests was largely driven by the expansion of agricultural land. The results show that the spatial distribution of forests, forest cover area, forest cover rate and deforestation rate vary greatly among different provinces.

## 2. Materials and Methods

### 2.1. Study Area and Data

#### 2.1.1. Study Area

The Federal Republic of Myanmar is the largest country in Southeast Asia. The north and northeast are bordered by Tibet and the Yunnan Province of China. The east side is adjacent to Laos and Thailand. The country covers an area of 676,578 km<sup>2</sup> and is divided administratively into seven divisions and seven states. The total population of Myanmar is 6.5 billion, ranked 25th in the world. The labor force is approximately 34.31 million, ranked 19th in the world. The terrain in Myanmar is relatively complex, with a maximum elevation of 6695 m and a minimum elevation of −547 meters relative to sea level. Myanmar is the country with the most abundant natural resources in the Indo-China Peninsula. Most of the area is at the south of the Tropic of Cancer and the south faces the ocean. It is regulated by the damp Indian Ocean in the southwest. Therefore, it belongs to the tropical monsoon climate and the south-central part is relatively hot. Central Myanmar is a dry area with an average annual precipitation of between 500 mm and 1000 mm. Coastal regions receive the largest amount of rainfall (over 5000 mm annually). Rainfall during the monsoon season totals more than 500 cm in upper Myanmar, and the annual precipitation in the delta and mountainous regions is between 2500 and 5000 mm. The terrain of Myanmar is shown in Figure 1 (due to the limitation of the length of the text in the picture, we used the uniform unit 'miles' as the size reference for the picture in the manuscript).

#### 2.1.2. Data

The socio-economic and demographic data were obtained through the World Bank. The Landsat datasets were downloaded from the United States Geological Survey (USGS) web site. Because of finite availability of satellite imagery data, we extracted them from different sensors including the Landsat5 Thematic Mapper (TM) (Landsat5, NASA, USA), the Landsat7 Enhanced Thematic Mapper Plus (ETM+) (Landsat7, NASA, USA), and the Landsat8 Operational Land Imager (OLI) (Landsat8, NASA,

USA). Table 1 provides an overview of the Landsat data. Moreover, a total of 43 scenes (Path: 129–135, Row: 40–53) for OLI/TM/ETM+ images were acquired to cover the entire study area. The wintertime data with visible snow was excluded by visual inspection. Since the study area is characterized by monsoon climate, it is difficult to obtain cloudless images during the rainy seasons, so that we only adopted two-month's data of a year: November (rainy season) and March (dry season). The best usable imagery data was selected based on phenology and cloud cover, where the cloud coverage should be less than 10%. Finally, a total of 387 remote sensing images across the study area were obtained. However, due to the variation of weather conditions, all the remote sensing data cannot be consistently obtained in the same day of different years, so that the remote sensing data of the same month of the previous year or the following year was obtained as supplementary data (Supplementary Material).

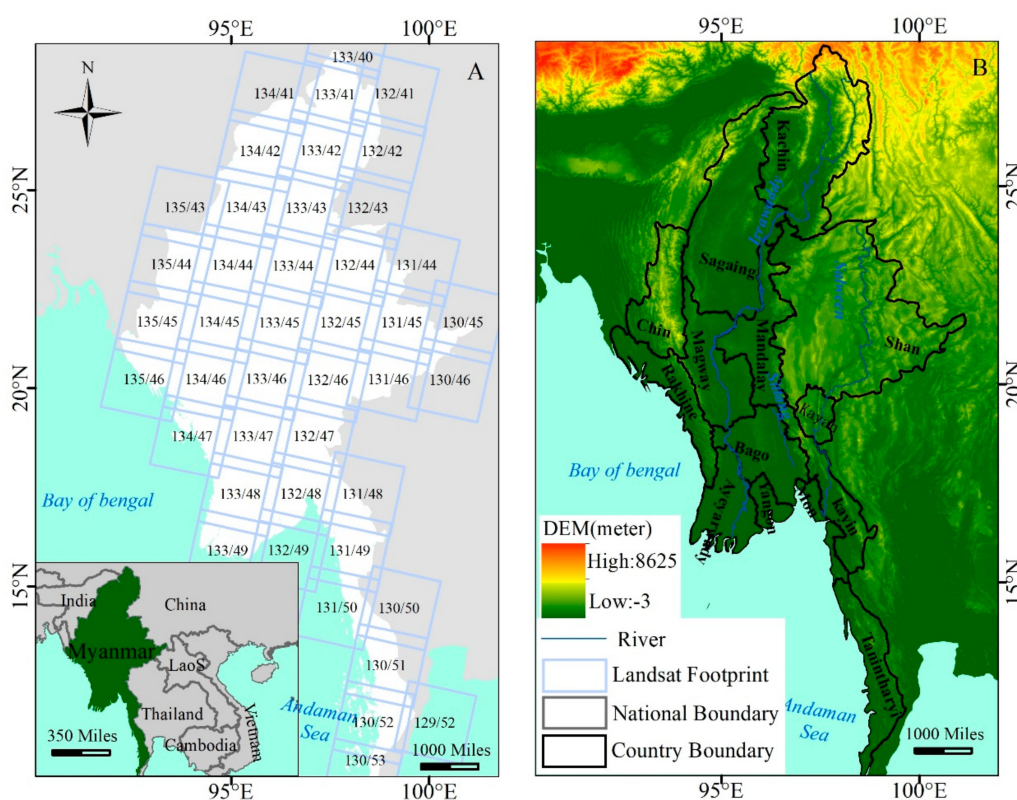


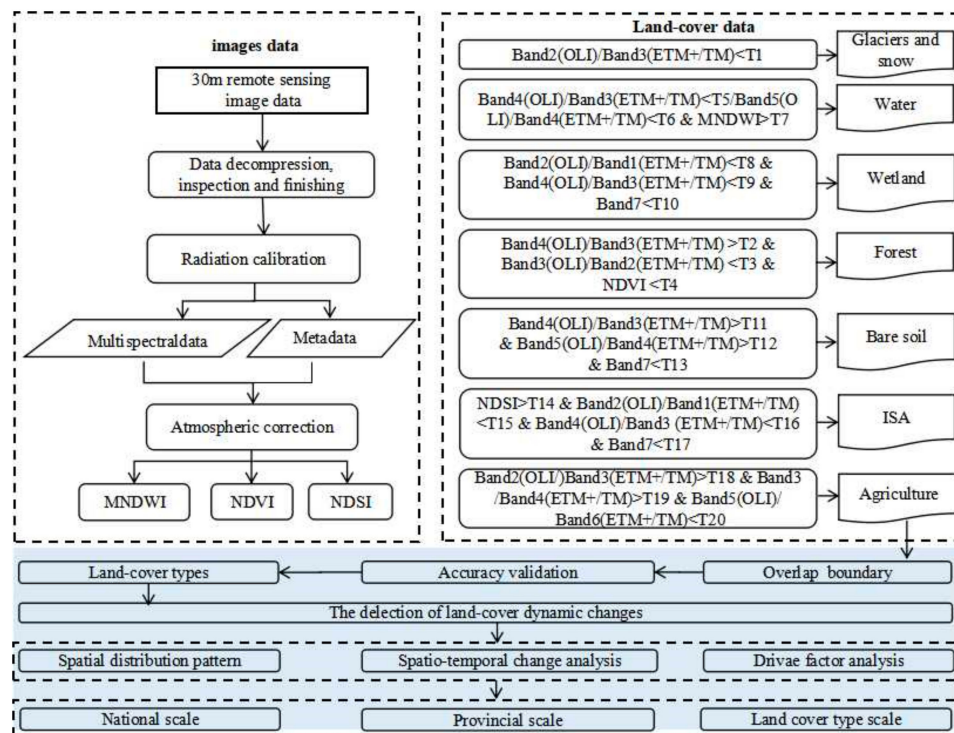
Figure 1. Study area. Notes: (A) Location and Landsat footprint; (B) terrain map.

Table 1. Landsat data used in this study.

Satellite Parameter	Landsat5		Landsat7		Landsat8	
Launch time	1984.3		1999.4.15		2013.2.11	
Coverage period	16 days		16 days		16 days	
Spatial resolution	30 m		30 m		30 m	
weep width	185 km		185 km		185 km	
sensor	MSS, TM		ETM+		OLI, TIRS	
Band	Name	Width ( $\mu\text{m}$ )	Name	Witdh ( $\mu\text{m}$ )	Name	Width ( $\mu\text{m}$ )
Band 1	Blue	0.45–0.52	Blue	0.45–0.52	Coastal	0.43–0.45
Band 2	Green	0.52–0.60	Green	0.52–0.60	Blue	0.45–0.51
Band 3	Red	0.63–0.69	Red	0.63–0.69	Green	0.53–0.59
Band 4	Near infrared	0.76–0.90	Near infrared	0.77–0.90	Red	0.64–0.67
Band 5	Mid-infrared1	1.55–1.75	Mid-infrared1	1.55–1.75	Near infrared	0.85–0.88
Band 6					Mid-infrared1	1.57–1.65
Band 7	Mid-infrared2	10.40–12.5	Mid-infrared2	2.09–2.35	Mid-infrared2	2.11–2.29

## 2.2. Methods

Figure 2 illustrates how to determine land cover classifications and how to detect land cover changes based on Landsat images. The Landsat remote sensing data with spatial resolution of 30 m were collated and analyzed, and the raster data were spliced and clipped to obtain the complete image data of the whole study area [36,37]. The data was radiometrically scaled based on ENVI software, after which the atmospheric calibration was performed on the data after radiometric calibration. According to band calculations, the normalized difference soil index (NDSI), the normalized difference vegetation index (NDVI), and the modified normalized difference water index (MNDWI) indices were further obtained. In the remote sensing image, the pixels with the pure land cover type were collected as the feature samples by visual interpretation [36], while the thresholds in the decision tree classifier were obtained by repeatedly training the feature samples.



**Figure 2.** Strategy for tracking land-cover dynamic changes by the use of Landsat data. Abbreviations: T1, T2, T3, T4, T5, T6, T7, T8, T9, T10, T11, T12, T13, T14, T15, T16, T17, T18, T19, T20, and T21: thresholds (the values of these quantities changed according to the different metrics used in the decision tree classifier); NDVI: normalized difference vegetation index; MNDWI: modified normalized Difference Water Index; NDSI: normalized difference soil index.

This paper adopts supervised classification to classify land cover types. In specific, we obtained data points of pure land cover categories from remote sensing images. These data points were further used as training samples to generate classification thresholds for each land cover category through repeated training automatically. Threshold obtained by the decision tree classification method was further adopted to distinguish land cover types. Afterwards, the hybrid matrix precision authentication method was adopted to evaluate the accuracy of our classifications. Afterwards, we superimposed the raster data onto the study area vector to extract the raster values. Then, statistical analysis of land cover classification area (area (km<sup>2</sup>) = number of pixels × 900 m<sup>2</sup>/1,000,000) from different scales (national boundaries, provincial boundaries) and the forest time change analysis were carried out based on the 30-year time series data. In the following subsections, we will explain each of these steps in detail.

### 2.2.1. Data Preprocessing

We conducted packet parsing of the raw data to obtain image information. In order to evaluate the quality of the original image, the first step was to visually inspect all Landsat images. After this, the data was preprocessed through radiation calibration and atmospheric calibration. The atmospheric correction was conducted based on the Fast line-of-sight atmospheric analysis spectral hypercubes (FLAASH) model. FLAASH, with the parameters of image center coordinates, sensor altitude, fast line of sight atmospheric analysis model, atmospheric model, and aerosol model, is a first-principles atmospheric calibration tool that corrects wavelengths in the visible through near-infrared and shortwave infrared regions [38].

### 2.2.2. Extraction of Index

Because of the existence of pixel mixing in the Landsat images, it is difficult to extract different land cover types accurately. For example, bare soil, glaciers and permanent snow, arable land and impervious surface area (ISAs) during fallow fall are characterized by high albedos, while, shadows, dark ISAs, wetlands and water have low albedos. Nevertheless, previous studies have shown that the NDSI can help separate ISA from high albedo types such as bare land and fallow arable land [39], and that the MNDWI can help separate water from low albedo types such as shadows and wetlands [40]. In addition to them, we further used the NDVI to separate water from shadows and wetlands. Based on these three indices, the accuracy of land cover classification could be improved. These three indices could be calculated according to Equations (1), (2) and (3), respectively. In the formula, NIR is the near infrared band, MIR1 is the Mid-infrared1 band and MIR2 is the Mid-infrared2.

$$NDSI = \frac{MIR2 - Green}{MIR2 + Green} \quad (1)$$

$$NDVI = \frac{NIR - Red}{NIR + Red} \quad (2)$$

$$MNDWI = \frac{Green - MIR1}{Green + MIR1} \quad (3)$$

### 2.2.3. Land-Cover Classification

The land cover in each scene would be divided into seven types, including forest, water, cropland, wetland, bare soil, ISA, glaciers and permanent snow cover, according to the approach presented in Ref [41]. During these steps, an appropriate threshold was generated according to the actual spectral characteristics of each image. Figure 3 shows the characteristics of different types exhibited by the remote sensing images (true color band combination), the superposition of raster data of different land cover types, and the classified vector data.

Based on the decision tree classification method, this paper extracted the 30-year land cover data of Myanmar. The classification and regression trees algorithm based on information theory is widely used as a decision tree classification method. The classification tree strategy uses the Gini index. The training feature set was prepared according to the visual interpretation of an ETM + image with reference to Google Earth (Windows, macOS, Linux; Google; Mountain View; United States of America). Pixels with a pure land cover type were selected as feature samples. Denote the training dataset as  $D$ , we then calculated the Gini index of the existing feature pair training dataset. For each feature  $A$ , the Gini index  $a$  was calculated when the training sample was cut into two parts,  $D1$  and  $D2$ , by feature  $A$ . For all possible features and all possible values, we selected the feature with the smallest Gini index and its segmentation point as the optimal feature and segmentation point, and we generated two child nodes, assigning the training dataset to its corresponding child node. In the model,

mathematical methods were used to build decision trees automatically, and decision trees were used to classify landmark types. When  $A = a$ , the Gini index was calculated according to Equation (4).

$$Gini(D, A) = \frac{|D1|}{D} Gini(D1) + \frac{|D2|}{D} Gini(D2) \quad (4)$$

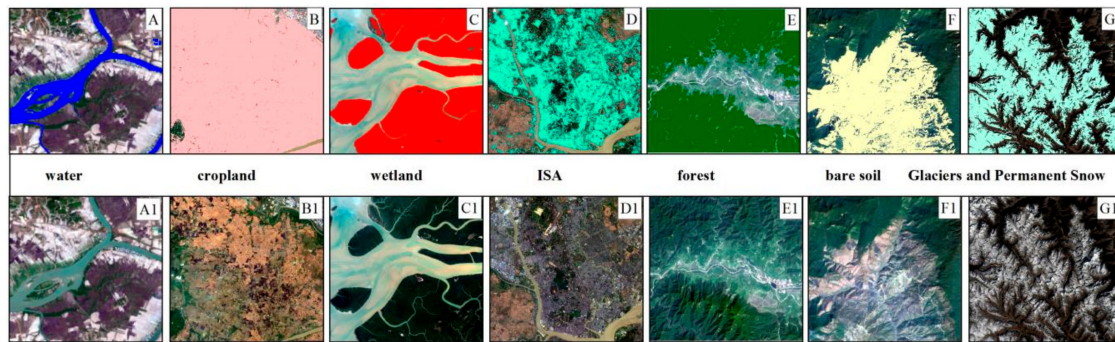


**Figure 3.** Characteristics of different land cover types presented by remote sensing images. Notes: Water, cropland, wetlands, ISA, forests, band soil and glaciers and permanent snow on the remote sensing image (true color band combination) are: **A, B, C, D, E, F, G**; the superimposed display of the raster data of the corresponding object type and the classified vector data is: **A1, B1, C1, D1, E1, F1, G1**.

Overall, different types of land cover present distinct spectral features. Water bodies on the spectrum usually exhibit a lower reflectance, and the reflectance gradually decreases as the wavelength increases. For many types of wetlands, their image features are complex because they are largely similar to vegetation. The spectral and texture characteristics of glaciers and permanent snow on an image are very stable. As a result, the glaciers and permanent snow cover of single scene images are easier to extract. In the 30 m resolution images, since the areas with impervious surface areas (ISAs) are usually small, most pixels are mixed with other natural objects, which increases the spectrum heterogeneity. Cropland has different characteristics depending on the growing season. In the case of false color band combination, the farmland in the growing season looks similar to vegetation, while the farmland after harvesting or fallow crops looks bright white. In terms of image characteristics, forest vegetation has obvious spectral characteristics and usually has a high vegetation index value. The bare soil spectrum is closely related to the characteristics of its inherent materials, and the texture features are mainly determined by geomorphological factors.

#### 2.2.4. Accuracy Evaluation Method

A confusion matrix can provide a basic description of the accuracy for thematic mapping [42]. Based on this, we evaluated the classification accuracy according to the overall accuracy and the kappa coefficient. In a matrix of  $n$  rows and  $n$  columns ( $n$  represents the number of categories), the evaluation indicators were calculated according to Equations (5) and (6) where  $x_{ij}$  is the number of classified samples in class  $i$  of classified data and class  $j$  of reference data,  $x_{i+}$  is the sum of category  $i$  of classified data,  $x_{+j}$  is the sum of category  $j$  of reference data,  $X_{kk}$  is the sum of data for each type of correct classification.  $N$  is the total number of evaluation samples.

$$\text{Overall Accuracy} = \frac{\sum_{k=1}^n x_{kk}}{N} \times 100 \quad (5)$$

$$\text{Kappa Coefficient} = \frac{N \sum_{i=1}^n x_{ij} - \sum_{i=1}^n x_{i+} x_{+i}}{N^2 - \sum_{i=1}^n x_{i+} x_{+i}} \quad (6)$$

### 3. Results

#### 3.1. Accuracy Analysis of Myanmar Land Cover Classification Results

This paper adopted the linear decomposition method to allocate 1000 sampling points, which helped avoid the mismatch between the sampling point number and land cover type. Wetlands, as well as the glaciers and permanent snow accounted for the smallest proportion of the study area, so that the assessment sample points of these two land cover types were added. The accuracy verification sample was prepared based on the visual interpretation of an ETM + image with reference to Google Earth. Among the data, the wetland sample number was the least (30 sample points), while the forest was the most with the number of 525.

The accuracy results are shown in Table 2. Nationally, the overall classification accuracy and kappa coefficient of land use in Myanmar ranged from 83% to 93% and from 0.801 to 0.904, respectively, between 1988 and 2017. ISA, bare soil and fallow arable land, forests, water and wetlands were more prone to mixed phenomena. This error is reasonable because the albedos of these features are similar.

**Table 2.** Data classification accuracy table.

Precision (%)	2017	2014	2011	2008	2004	2000	1996	1992	1988
Overall Accuracy (%)	93.61	91.74	89.87	88.93	89.77	90.61	83.31	86.12	85.18
Kappa Coefficient (%)	90.40	88.24	86.44	85.54	86.35	87.16	80.14	82.84	81.94

#### 3.2. Spatial and Temporal Distribution of Forest and Its Changing Characteristics

Deforestation assessment plays a crucial role in sustainable management. Information related to forest cover change can inform researchers and the government with the deforestation situation in Myanmar. Results show that the spatial distribution of land cover in Myanmar is very uneven at present. Croplands are predominantly in the dryer central region, while forests are mainly distributed in the surrounding areas. The forest distribution in the north and south direction is more intensive. High-altitude areas have limited the logging activity, so that we did not observe obvious forest loss in Sagaing. In Yangon, Mon and Ayeyarwady provinces, because of the rapid expansion of arable land, the forest area had been sharply reduced, while the forest variations in other provinces were relatively stable. During the period of 1988–2017, the forest area of Yangon, Mon, and Ayeyarwady decreased by 59%, 58% and 39%, respectively, while the cropland area increased by 18%, 70% and 39%, respectively. This polarization can be partly explained by the increasing resource demands of a large population in the central region, a decline in the national control of forest resources, and the barrier of remote high altitudes to logging activity. Myanmar witnesses a much slower deforestation than other countries (e.g., Indonesia and Vietnam) in the Southeast Asia, but forest loss remains to be an important environmental issue.

It is worth noting that the spatial distribution, coverage area, coverage rate and deforestation rate of forests varied significantly among different provinces during the study period. The spatial distribution of forests in Magway, Mandalay and Yangon was extremely uneven. Ayeyarwady had the highest annual average deforestation rate (1.99%), the 11th annual average forest cover area (6756 km<sup>2</sup>) and the 12th forest cover (20%). Chin State had the highest annual average forest cover and the fourth the annual average forest coverage area. Shan State had the largest annual average forest cover area (85,439 km<sup>2</sup>), and the seventh the forest cover (54%). Yangon Province had the smallest annual average forest cover area (989 km<sup>2</sup>) and forest cover (10%), but the annual average deforestation rate ranked second. The annual average forest cover in Tanintharyi (86%), Kachin (81%), and Chin (80%) far exceeded the national level (55%). The annual average forest cover in Yangon (10%), Magway (18%), and Ayeyarwady (20%) far lower than the national level. Mon (1.75%), Ayeyarwady (1.99%) and Yangon (1.96%) were the three regions with the highest rates of deforestation.

### 3.2.1. Spatial and Temporal Forest Distribution

Figure 4 shows the spatial distribution of forests in Myanmar from 1988 to 2017. It exhibits that the spatial distribution of forests in Myanmar is uneven, with forests mainly in the surrounding areas while cropland in the central areas. According to the spatial map of forest presented in Figure 4, there are significant differences in the spatial patterns of forests among different provinces. The spatial patterns of forests in the Yangon, Mandalay, Ayeyarwady, and Magway Provinces are similar: forest cover is limited and unevenly distributed. The forest cover in the Kachin, Chin, Tanintharyi, and Kayah States is much higher and more evenly distributed. Forests in the Yangon Province have gradually decreased from north to south, while in the Magway and Ayeyarwady Provinces, forests have gradually decreased from west to east. Permanent snow and glaciers are mainly distributed in the high-altitude Kachin State area.

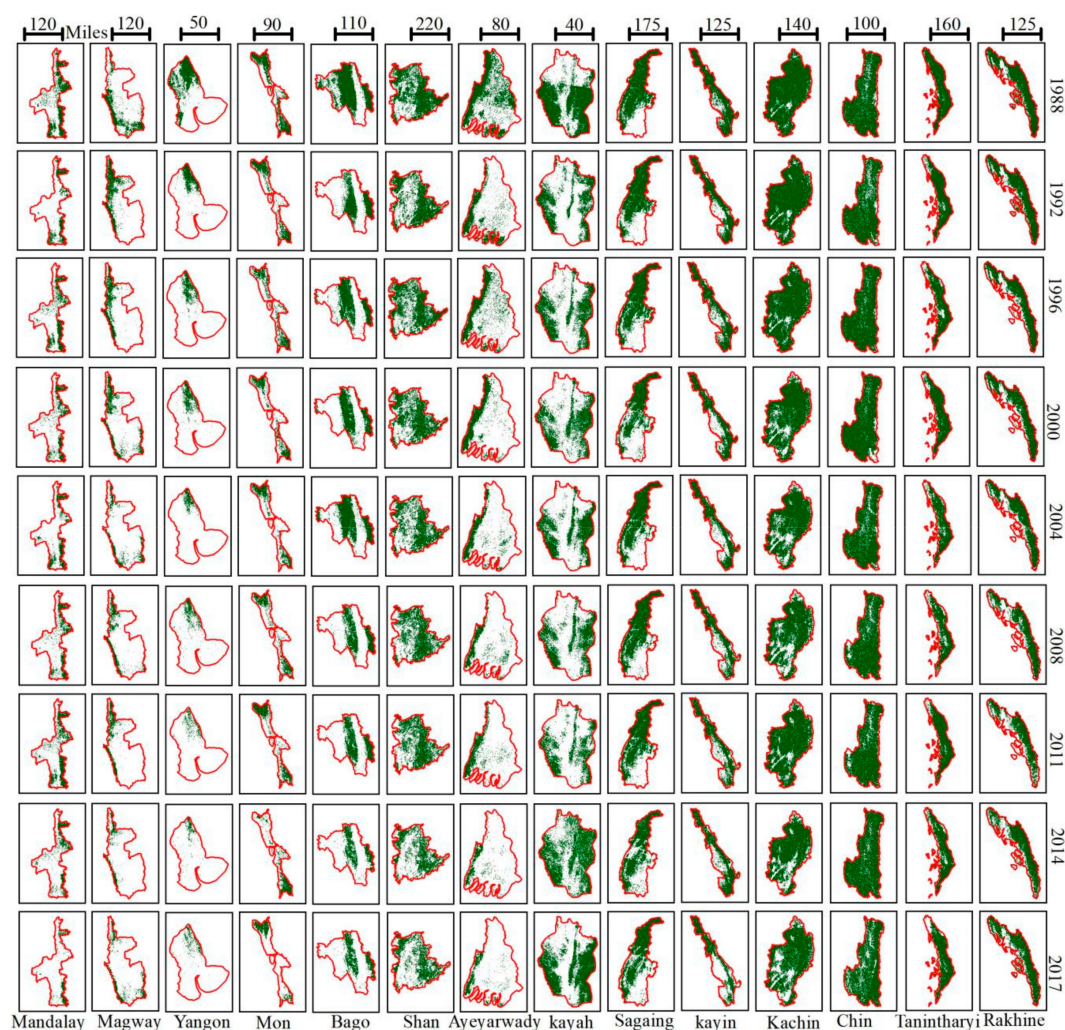


**Figure 4.** Spatial distribution of forests from 1988 to 2017.

The distribution of forests in Myanmar across different periods is shown in Table 3. During the study period, the forest area in Myanmar dropped sharply from 438,653 km<sup>2</sup> in 1988 (65% of the country's land area) to 338,033 km<sup>2</sup> in 2017 (48% of the country's land area). Among them, Kachin State underwent the highest loss in forest area (18,459 km<sup>2</sup>), and Magway and Kayah did the lowest at 597 km<sup>2</sup> and 740 km<sup>2</sup>, respectively. The forest areas of the Chin State increased by 893 km<sup>2</sup>. The forest covers of Tanintharyi, Chin, Rakhine, Kachin and Kayah at 88%, 87%, 76%, 92%, and 82%, were higher than the nationwide forest coverage level consistently. Forest covers in Mandalay, Marquee, and Yangon were low at 22%, 24% and 27%, respectively. Yangon is the largest city in Myanmar with a land area of

9279 km<sup>2</sup>, of which cropland accounts for more than 70%. Nevertheless, its forest cover were keeping shrinking during the period of 1988–2008, but then increased significantly from 2008 to 2017.

**Table 3.** Forestry Coverage Area of Provinces in Myanmar (unit:10,000 km<sup>2</sup>).

Province/State	1988	1992	1996	2000	2004	2008	2011	2014	2017
Yangon	0.26	0.11	0.09	0.08	0.05	0.06	0.04	0.02	0.02
Kayah	0.62	0.44	0.41	0.41	0.40	0.39	0.37	0.35	0.28
Magway	1.08	1.01	0.92	0.80	0.69	0.63	0.59	0.51	0.47
Ayeyarwady	1.21	1.00	0.97	0.72	0.57	0.47	0.49	0.33	0.32
Mon	0.60	0.45	0.45	0.38	0.37	0.40	0.44	0.33	0.29
Bago	2.25	1.76	1.56	1.25	1.22	1.31	1.22	1.16	0.91
Mandalay	2.90	2.69	2.78	2.64	2.57	2.48	2.39	2.24	2.13
Chin	3.41	3.34	3.27	3.36	3.36	3.21	3.21	3.17	2.97
Kayin	2.48	2.12	2.18	2.05	2.06	1.93	1.91	1.92	1.51
Rakhine	2.70	2.63	2.41	2.34	2.32	2.25	2.22	2.04	1.94
Tanintharyi	3.61	3.34	3.26	3.10	3.21	3.07	3.09	3.04	2.94
Sagaing	6.36	5.96	5.89	5.91	5.79	5.63	5.27	5.13	5.00
Kachin	8.23	8.19	8.02	7.83	7.83	7.78	7.77	7.51	7.42
Shan	9.94	9.60	9.27	8.88	8.47	8.35	8.25	7.45	6.69

### 3.2.2. Forest Cover Dynamics between 1988 and 2017

In the past three decades, the spatial coverage of forests in Myanmar has been decreasing, while agricultural land has been increasing. The dynamics of forests in Myanmar during the study period are shown in Figure 5. The most significant change occurred between 1988 and 1992, with a net forest area reduction of 51,089 km<sup>2</sup> and an annual average deforestation rate of 4.15%. During the periods of 2000–2004 and 2014–2017, Myanmar underwent its lowest annual deforestation, with the area reductions of 1938 km<sup>2</sup> and 1190 km<sup>2</sup>, respectively. During the period of 1988–2017, the nationwide forest cover decreased from 438,653 km<sup>2</sup> in 1988 to 338,033 km<sup>2</sup> in 2017, namely the forest cover decreased from 65% to 48%. The cropland area increased from 188,694 km<sup>2</sup> in 1988 to 257,880 km<sup>2</sup> in 2017, with a total growth area of 69,185 km<sup>2</sup>. It is worth noting that the most significant expansion of cropland also occurred between 1988 and 1992, with a total increase of 58,365 km<sup>2</sup>. The ISA expanded from 295 km<sup>2</sup> in 1988 to 3814 km<sup>2</sup> in 2017, with an average annual growth rate of 41%. During the period of 1988–2017, the newly added forest area was 3618 km<sup>2</sup>. Nevertheless, across different periods, there was no apparent difference in the newly added forest area.

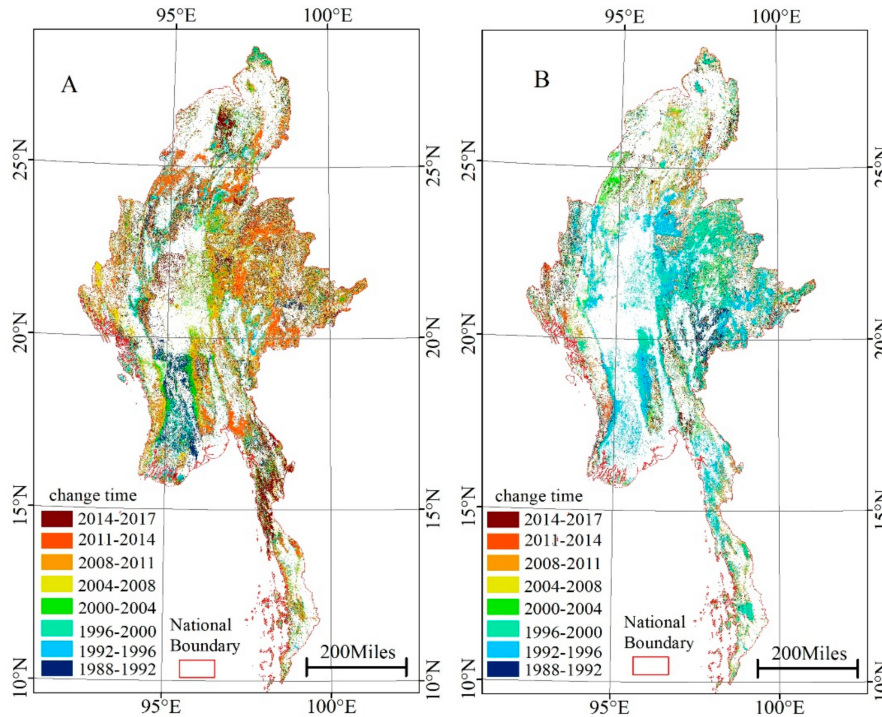
### 3.2.3. Forest Cover Transfer Characteristic

This study analyzed the conversion among different land cover types in Myanmar over a 30-year period. Meanwhile, the conversion between different land cover types and forest cover was also concerned. According to the 30 m resolution land cover data, the confusion matrix of land cover classifications in two phases were calculated in terms of a cross-tabulation matrix. The transfer matrix results of different land cover types were analyzed, and the changes of land cover types from 1988 to 2017 was detected by a confusion matrix (Figure 6), in which the expansion of cropland led to the fragmentation of adjacent forests.

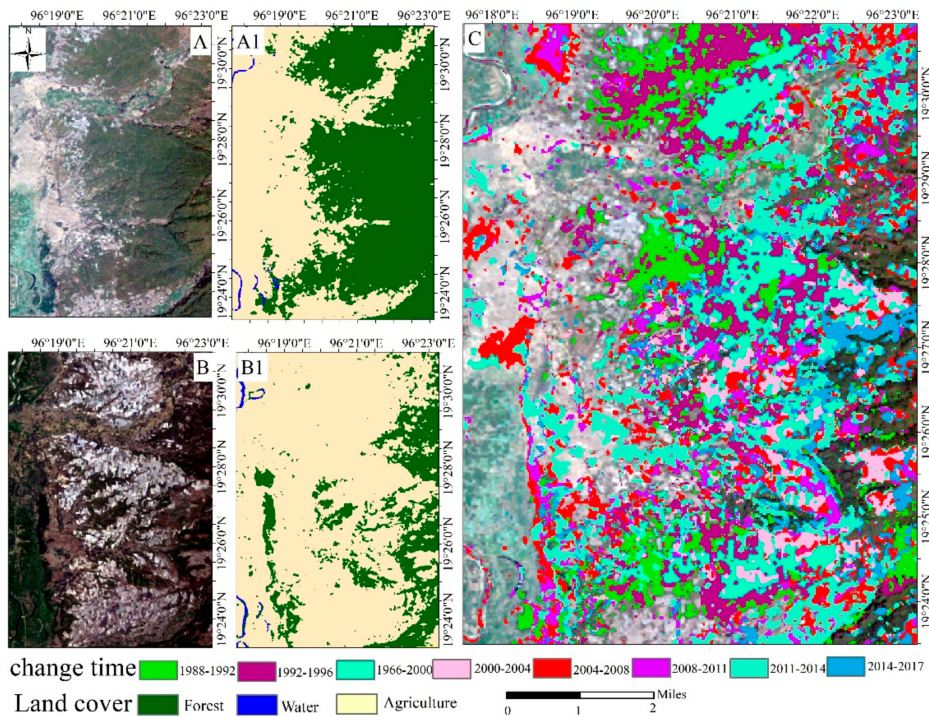
### 3.2.4. Deforestation Rates between 1988 and 2017

Figure 7 illustrates the forest cover (A) and the annual average deforestation rate (B) of each administrative division. It is indicated that the total forest loss in Myanmar over the past 30 years was 110,621 km<sup>2</sup>, and the annual average loss rate of forests was 0.87%. During the same study period, there was about 36,182 km<sup>2</sup> of forest regeneration, to some extent alleviating the annual forest loss rate. From 1988 to 2017, all states and provinces suffered from a certain degree of deforestation, except for Sagaing and Chin. In the past three decades, the average annual deforestation rates of Ayeyarwady

and Yangon were 1.99% and 1.96%, respectively, about twice as fast as the nationwide deforestation rate. Ayeyarwady, Yangon and Mon had the highest annual deforestation rates, but these provinces showed a relatively small reduction in forest area. Kachin State had the largest forest area with a total area of 18,459 km<sup>2</sup>.



**Figure 5.** Spatial Dynamic Change of Forest in Myanmar from 1988 to 2017 ((A): reduction in forest area; (B): increase in forest area).



**Figure 6.** Spatial subset true color remote sensing image map (A) 1988; (B) 2017, spatial subset land cover classification map; (A1) 1988, spatial subset land cover classification map; (B1) 2017, land cover classification change pixels; (C) in different research periods.

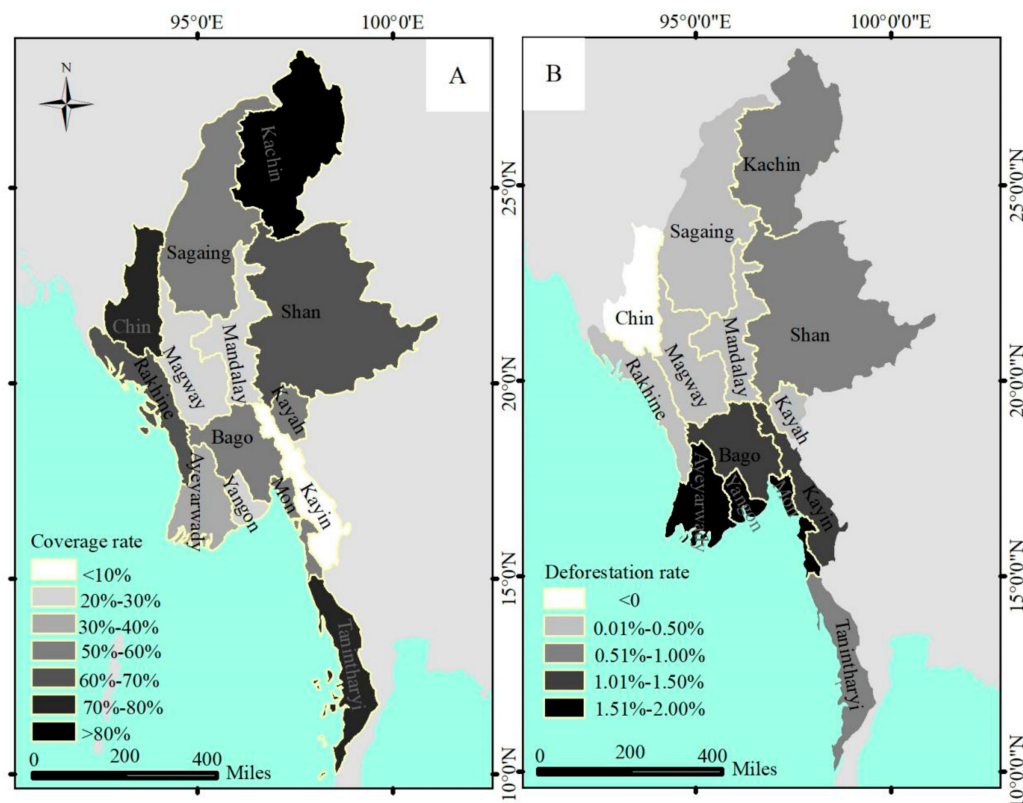


**Figure 7.** Percentage of forest cover map (A); and Mean annual deforestation rate map (B) for Myanmar between 1988 and 2017. Negative numbers denote afforestation, and positive numbers indicate deforestation.

During the period from 1988 to 1992, the forest loss was the most serious. The total forest loss was 51,088 km<sup>2</sup>, and the annual average deforestation rate was 2.91%. The second worst period was from 1992 to 1996, during which time the forest loss area was 17,143 km<sup>2</sup>. During other periods, the area of deforestation was less than 10,000 km<sup>2</sup>. The area of cropland continued to expand from 1988 to 2017, with its proportion increase of 10 percent from 28% in 1988 to 38% in 2017. Through examining the past 30-year forest change, it is found about 70% forest area was well reserved, not affected by the land cover changes.

### 3.3. Driving Forces of Forest deforestation

This section presents the causes of the deforestation across the country. Histogram of mutual change between different land cover types is presented in Figure 8. During the period of 1988–2017, the deforestation area caused by the expansion of agricultural land, urban expansion and bare land was 91,033 km<sup>2</sup>, 1015 km<sup>2</sup> and 25,136 km<sup>2</sup>, respectively. This indicates the expansion of the agricultural land was the first culprit of the deforestation in Myanmar, followed by bare land and urban expansion. The trend indicates the rapid needs for agricultural land to feed the increasing population. Nevertheless, the land ruin after the human caused deforestation (about 20%) should be highly concerned in the future. Urban expansion was also important factors for forest deforestation. With the future urbanization, the influence of urban expansion will be aggravated. Moreover, the ongoing new and rapid economic transformations can also make the protection of forest ecosystems become increasingly difficult. Overall, this helps determine the future concerns of the Myanmar government in the massive and rapid agricultural investment, the demand of Myanmar neighboring countries for raw wood materials and agricultural products, as well as the future urbanization and infrastructure construction.

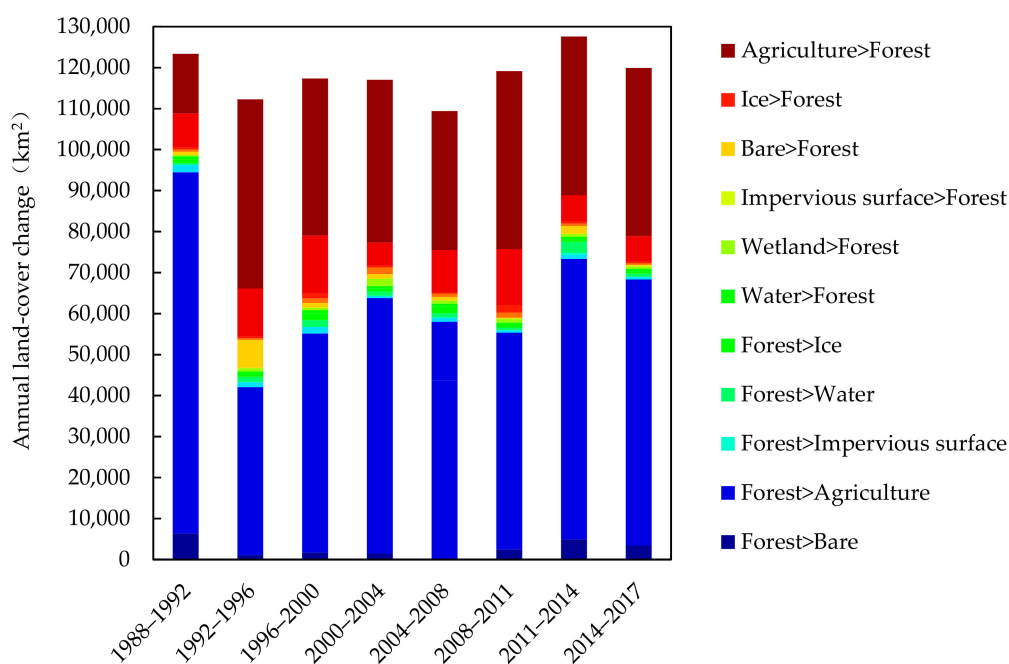


**Figure 8.** Histogram of the annual amounts (km<sup>2</sup>) of different kinds of forest-related land cover change between 1988 and 2017.

#### 4. Discussion

This study showed that 30% of the forest cover changed during the period of 1988–2017, and the total loss of forest area was 110,621 km<sup>2</sup>. Throughout this period, the rate of deforestation varied greatly. The annual average forest loss area is 12,772 km<sup>2</sup> during the period of 1988–1992, 24,248 km<sup>2</sup> during the period of 1992–1996, 3,570 km<sup>2</sup> during the period of 1996–2000, and 3570 km<sup>2</sup> during the period of 2004–2008. Comparatively, the annual average forest loss area between 2000 and 2011 was less than 1500 km<sup>2</sup>. From 1988 to 1992, the annual deforestation rate was the highest and the area of deforestation was the largest. Myanmar’s economic and politic background can help explain the patterns of deforestation observed in this study. Major economic changes in the country occurred in 1988, resulting in many families losing their savings and being forced to rely more heavily on the exploitation of forest resources. Myanmar has experienced a process of rapid deforestation driven by agriculture [13,43]. Moreover, the spatial distribution of forests was continuously fragmented by the expansion of agricultural land across the study period. The transition from connected forest areas to smaller and fragmented patches occurred. About 74% of the lost forest area was replaced by agricultural land. Large-scale and rapid agricultural investment should attract some attention of the Myanmar government.

This study has some limitations. The land cover classification based on 30 m spatial resolution cannot fully represent the results obtained by high-resolution image interpretation. Changes in vegetation greenness may occur because of climate fluctuations, but the forest area is not affected. Combinations based on pixel classification and index image information extraction are critical in this study. The surface features of the study area are very complex. For example, the spectral characteristics of agricultural land in the fallow period are akin to those of bare soil and buildings. In addition, some agricultural land has two farming periods within one year, which increases the difficulty of data acquisition and classification of features. Through phenological analysis and post-classification processing, the classification accuracy is improved. In the classification process, based on the classification of the decision tree, it is necessary to continuously debug the threshold according to the classification result and repeatedly obtain the optimal classification threshold. The use of a consistent classification approach in this paper is the key to ensure the comparability of the results

over time. The results pointed out a net forest loss of 110,621 km<sup>2</sup> countrywide, and an annual average deforestation rate of 0.87% between 1988 and 2017. This deforestation rate is lower than that reported in the Food and Agriculture Organizations of the United Nations 2010 report (0.93%) [10]. This is the result of a study using different data sets and different methods to assess forest degradation. This study used Landsat remote sensing imagery to produce forest maps, showing that forest estimation accuracy was higher due to its high spatial resolution and cloudless observations. This study can provide reference for other experts in the field to carry out other regional and land use classification, forest coverage degradation driver analysis and other related research.

## 5. Conclusions

The purpose of this study was to provide an up-to-date and consistent overview of recent deforestation patterns in Myanmar. Based on remotely sensed Landsat data with a spatial resolution of 30 m, forest mapping in Myanmar from 1988 to 2017 was completed. According to the change of forest cover in the past 29 years, the areas of forest cover reduction and increase were identified. The annual average loss information was provided, and forest loss trends were quantified. Two spatial scales (i.e., nationwide and province wide) of forest coverage patterns were presented in the form of maps. A comprehensive assessment of the agricultural land expansion indicated that forest loss was largely driven by the expansion of agricultural land in Myanmar. Myanmar is experiencing rapid deforestation and has a high risk of forest loss, with the annual average forest loss rate of 0.87%. The annual average deforestation rates in Ayeyarwady, Yangon, and Mon were higher than the nationwide average. The forest cover of Kachin, Chin, Kayin, and Tanintharyi were extremely high, all exceeding 80%. The spatial deforestation rate and spatial coverage of Myanmar forests varied widely from province to province. Kachin State had the highest forest coverage, and Tanintharyi had the largest forest cover area. Forest loss was more serious in low-latitude areas with fast economic development, dense population and concentrated arable land. Yangon Province had the smallest forest coverage and its annual average deforestation rate ranked second. There is almost no loss of forest cover in Sagaing.

With the development of remote sensing technology and the increasing data availability of fine-resolution images, there are new possibilities of rebuilding land cover history for decades. In view of this, a novel and more systematic change detection method is needed to fully determine the temporal pattern of the land cover change. This study thus reports on the initial attempts to analyze the temporal and spatial characteristics of the deforestation process. The applied method can prove the forest coverage trajectory change pattern and has the ability to directly detect the potential causes of the change. Providing information on the processes and potential drivers of forest change is conducive to identifying hotspots of forest loss. The maps and statistics provide a preliminary reference for Myanmar to promote national forest protection and management.

**Supplementary Materials:** The following are available online at <http://www.mdpi.com/2071-1050/11/11/3047/s1>; Figure S1: Research on data cloud coverage, Figures S2–S8: Land cover change curve from 1988 to 2017, Figures S9–S22: The spatial distribution of forests in the provinces of Myanmar from 1988 to 2017, Table S1: Interchange between forest and other land use types (unit: km<sup>2</sup>), Table S2: Data detail table, Table S3: Accuracy of land use classification, Table S4: Mutual transformation between land cover types from 1988 to 2017 (unit: Pixel Counts).

**Author Contributions:** Y.L. and K.Y. designed and performed this research; R.Y., L.H. analyzed the data and performed the experiments; R.Y. drafted the manuscript; X.Z. edited the manuscript.

**Funding:** This research was funded by National Natural Science Foundation of China (41761084), China High Technology Research and Development Program 863 (2012AA121402) and Yunnan Natural Science Foundation of China (2016FD020).

**Conflicts of Interest:** The authors declare no conflict of interest.

## References

1. Foley, J.A. Atmospheric science. Tipping points in the tundra. *Science* **2005**, *310*, 627. [[CrossRef](#)]

2. Alkama, R.; Cescatti, A. Biophysical climate impacts of recent changes in global forest cover. *Science* **2016**, *351*, 600–604. [[CrossRef](#)] [[PubMed](#)]
3. Gullison, R.E.; Frumhoff, P.C.; Canadell, J.G. Tropical Forests and Climate Policy. *Science* **2007**, *316*, 985–986. [[CrossRef](#)]
4. Yang, K.; Yu, Z.; Luo, Y. Spatial and temporal variations in the relationship between lake water surface temperatures and water quality—A case study of Dianchi Lake. *Sci. Total Environ.* **2018**, *624*, 859–871. [[CrossRef](#)] [[PubMed](#)]
5. Feddema, J.J. The Importance of Land-Cover Change in Simulating Future Climates. *Science* **2005**, *310*, 1674–1678. [[CrossRef](#)] [[PubMed](#)]
6. Lawrence, D.; Vandecar, K. Effects of tropical deforestation on climate and agriculture. *Nat. Clim. Chang.* **2014**, *5*, 27–36. [[CrossRef](#)]
7. Achard, F.; Eva, H.D.; Stibig, H.-J. Determination of deforestation rates of the world’s humid tropical forests. *Science* **2002**, *297*, 999–1002. [[CrossRef](#)] [[PubMed](#)]
8. Wilcove, D.S.; Giam, X.; Edwards, D.P. Navjot’s nightmare revisited: Logging, agriculture and biodiversity in Southeast Asia. *Trends Ecol. Evol.* **2013**, *28*, 531–540. [[CrossRef](#)]
9. Tropek, R.; Sedláček, O.; Beck, J. Comment on Comment on “High-resolution global maps of 21st-century forest cover change”. *Science* **2014**, *344*, 981. [[CrossRef](#)] [[PubMed](#)]
10. FAO. *Global Forest Resources Assessment 2000 (FRA 2000)*; Food and Agriculture Organizations of the United Nations: Rome, Italy, 2000.
11. Songer, M.; Aung, M.; Senior, B. Spatial and temporal deforestation dynamics in protected and unprotected dry forests: A case study from Myanmar (Burma). *Biodiver. Conserv.* **2009**, *18*, 1001–1018. [[CrossRef](#)]
12. Bhagwat, T.; Hess, A.; Horning, N. Losing a jewel—Rapid declines in Myanmar’s intact forests from 2002–2014. *PLoS ONE* **2017**, *12*, e0176364. [[CrossRef](#)]
13. Chuyuan, W.; Soe, M. Environmental Concerns of Deforestation in Myanmar 2001–2010. *Remote Sens.* **2016**, *8*, 728. [[CrossRef](#)]
14. Mon, M.S.; Mizoue, N.; Htun, N.Z. Factors affecting deforestation and forest degradation in selectively logged production forest: A case study in Myanmar. *For. Ecol. Manag.* **2012**, *267*, 190–198. [[CrossRef](#)]
15. Leimgruber, P.; Kelly, D.S.; Steininger, M.K. Forest cover change patterns in Myanmar (Burma) 1990–2000. *Environ. Conserv.* **2005**, *32*, 356. [[CrossRef](#)]
16. Webb, E.L.; Jachowski, N.R.A.; Phelps, J. Deforestation in the Ayeyarwady Delta and the conservation implications of an internationally-engaged Myanmar. *Glob. Environ. Chang.* **2014**, *24*, 321–333. [[CrossRef](#)]
17. Renner, S.C.; Rappole, J.H.; Leimgruber, P. Land cover in the Northern Forest Complex of Myanmar: New insights for conservation. *Oryx* **2007**, *41*, 27–37. [[CrossRef](#)]
18. Htun, N.Z.; Mizoue, N.; Kajisa, T. Deforestation and forest degradation as measures of Popa Mountain Park (Myanmar) effectiveness. *Environ. Conserv.* **2009**, *36*, 218. [[CrossRef](#)]
19. Sexton, J.O.; Noojipady, P.; Song, X.P. Conservation policy and the measurement of forests. *Nat. Clim. Chang.* **2015**, *6*. [[CrossRef](#)]
20. Wulder, M.A.; Masek, J.G.; Cohen, W.B. Opening the archive: How free data has enabled the science and monitoring promise of Landsat. *Remote Sens. Environ.* **2012**, *122*, 2–10. [[CrossRef](#)]
21. Hassan, M.M. Monitoring land use/land cover change, urban growth dynamics and landscape pattern analysis in five fastest urbanized cities in Bangladesh. *Remote Sens. Appl. Soc. Environ.* **2017**, *7*, 69–83. [[CrossRef](#)]
22. Turner, W.; Spector, S.; Gardiner, N. Remote sensing for biodiversity science and conservation. *Trends Ecol. Evol.* **2003**, *18*, 306–314. [[CrossRef](#)]
23. Moran, E.F.; Brondizio, E.; Mausel, P. Integrating Amazonian Vegetation, Land-Use, and Satellite Data. *Bioscience* **1994**, *44*, 329–338. [[CrossRef](#)]
24. Steininger, M.K. Tropical secondary forest regrowth in the Amazon: Age, area and change estimation with Thematic Mapper data. *Int. J. Remote Sens.* **1996**, *17*, 9–27. [[CrossRef](#)]
25. Kun, Y.; Meie, P.; Yi, L. A time-series analysis of urbanization-induced impervious surface area extent in the Dianchi Lake watershed from 1988–2017. *Int. J. Remote Sens.* **2018**, *40*, 1–20. [[CrossRef](#)]
26. Bryant, R. *The Political Ecology of Forestry in Burma 1824–1994*; University of Hawaii Press: Honolulu, HI, USA, 1997.

27. Seekins, D.M. *Historical Dictionary of Burma (Myanmar), Historical Dictionaries of Asia, Oceania, and the Middle East*, No. 59; The Scarecrow Press, Inc: Lanham, MD, USA, 2006.
28. Pimm, S.L.; Jenkins, C.N.; Abell, R. The biodiversity of species and their rates of extinction, distribution, and protection. *Science* **2014**, *344*. [[CrossRef](#)]
29. Myers, N.; Mittermeier, R.A.; Mittermeier, C.G. Biodiversity hotspot for conservation priorities. *Nature* **2000**, *403*, 853–858. [[CrossRef](#)]
30. Barbier, E.B. Explaining Agricultural Land Expansion and Deforestation in Developing Countries. *Am. J. Agric. Econ.* **2004**, *86*, 1347–1353. [[CrossRef](#)]
31. Yearley, S.; Kugelman, M. The global farms race: Land grabs, agricultural investment, and the scramble for food security. *Food Secur.* **2013**, *5*, 613–614. [[CrossRef](#)]
32. Zhang, Y.; Prescott, G.W. Dramatic cropland expansion in Myanmar following political reforms threatens biodiversity. *Nature* **2018**, *8*. [[CrossRef](#)] [[PubMed](#)]
33. Yang, K.; Yu, Z.; Luo, Y. Spatial-Temporal Variation of Lake Surface Water Temperature and its Driving Factors in Yunnan-Guizhou Plateau. *Water Resour. Res.* **2019**, *55*. [[CrossRef](#)]
34. Kim, D.H.; Sexton, J.O.; Townshend, J.R. Accelerated deforestation in the humid tropics from the 1990s to the 2000s. *Geophys. Res. Lett.* **2015**, *42*, 3495–3501. [[CrossRef](#)]
35. Webb, E.L.; Phelps, J.; Friess, D.A. Environment-friendly reform in Myanmar. *Science* **2012**, *336*, 295. [[CrossRef](#)]
36. Zhao, Z.Q.; He, B.J.; Li, L.G.; Wang, H.B.; Darko, A. Profile and concentric zonal analysis of relationships between land use/land cover and land surface temperature: Case study of Shenyang, China. *Energy Build.* **2017**, *155*, 282–295. [[CrossRef](#)]
37. He, B.J.; Zhao, Z.Q.; Shen, L.D.; Wang, H.B.; Li, L.G. An approach to examining performances of cool/hot sources in mitigating/enhancing land surface temperature under different temperature backgrounds based on landsat 8 image. *Sust. Cities Soc.* **2019**, *44*, 416–427. [[CrossRef](#)]
38. Rani, N.; Mandla, V.R.; Singh, T. Evaluation of atmospheric corrections on hyperspectral data with special reference to mineral mapping. *Geosci. Front.* **2017**, *8*, 797–808. [[CrossRef](#)]
39. Deng, Y.; Wu, C.; Li, M.; Chen, R. RNDI: A ratio normalized difference soil index for remote sensing of urban/suburban environments. *Int. J. Appl. Earth Obs. Geoinf.* **2015**, *39*, 40–48. [[CrossRef](#)]
40. Han-Qiu, X.U. A Study on Information Extraction of Water Body with the Modified Normalized Difference Water Index (MNDWI). *J. Remote Sens.* **2005**, *9*, 589–595. [[CrossRef](#)]
41. Chen, J.; Chen, J.; Liao, A.; Cao, X.; Chen, L.; Chen, X.; He, C.; Han, G.; Peng, S.; Lu, M.; et al. Global land cover mapping at 30 m resolution: A POK-based operational approach. *ISPRS J. Photogramm. Remote Sens.* **2015**, *103*, 7–27. [[CrossRef](#)]
42. Foody, G.M. Status of land cover classification accuracy assessment. *Remote Sens. Environ.* **2002**, *80*, 185–201. [[CrossRef](#)]
43. Huggett, R.B.R. *The Earth as Transformed by Human Action: Global and Regional Changes in the Biosphere over the Past 300 Years*; Turner, B.L., Clark, W.C., Kates, R.W., Richards, J.F., Mathews, J.T., Meter, W.B., Eds.; Cambridge University Press: Cambridge, UK, 1993; 732p.

